

Pattern formation induced by nonequilibrium global alternation of dynamics

J. Buceta and Katja Lindenberg

Department of Chemistry and Biochemistry and Institute for Nonlinear Science, University of California, San Diego, 9500 Gilman Drive, La Jolla, California 92093-0340

J. M. R. Parrondo

Departamento de Física Atómica, Molecular y Nuclear, Universidad Complutense de Madrid, Ciudad Universitaria s/n, 28040 Madrid, Spain

(Received 13 February 2002; published 24 September 2002)

We recently proposed a mechanism for pattern formation based on the alternation of two dynamics, neither of which exhibits patterns. Here we analyze the mechanism in detail, showing by means of numerical simulations and theoretical calculations how the nonequilibrium process of switching between dynamics, either randomly or periodically, may induce both stationary and oscillatory spatial structures. Our theoretical analysis by means of mode amplitude equations shows that all features of the model can be understood in terms of the nonlinear interactions of a small number of Fourier modes.

DOI: 10.1103/PhysRevE.66.036216

PACS number(s): 05.45.-a, 47.54.+r, 89.75.Kd

I. INTRODUCTION

Spatiotemporal pattern formation in nonequilibrium extended systems plays a role in a huge number of physical phenomena, and in the past few decades there has been continuous progress in the understanding of different mechanisms that lead to such patterns. The mechanisms for pattern formation that have been studied most thoroughly and invoked most frequently include dissipative structures, often involving an input of heat balanced by dissipation, or chemical oscillations in dissipative open systems [1]. Other well-known cases involve patterns formed by the temporal modulation of a parameter in systems that undergo Hopf bifurcations [2,3], and noise-induced patterns [4,5].

In recent work we introduced a new mechanism for spatial and spatiotemporal pattern formation induced by a *global* alternation between two dynamics, each of which by itself leads to a spatially homogeneous state [6,7]. When the alternation is periodic [6] the spatial patterns are stationary in some parameter regimes and oscillatory (reminiscent of oscillons in granular materials [8]) in others. Random alternation leads to stationary patterns [7].

We note that there are many nonlinear spatially distributed systems in which external forcing leads to pattern formation, pattern selection, pattern stabilization, appearance of coherent structures, and other ordering effects. The external forcing may be constant (dc forcing), random (temporally and/or spatially), or periodic (again, temporally and/or spatially). The literature on *global* forcing (i.e., space-independent forcing such as that considered in this paper) usually focuses on periodic modulation. A few representative examples include parametric pumping of electrons in a Penning trap which can lead to coherent collective phase-bistable motion of the electrons' center of mass [9], breather stabilization in a sine-Gordon system [10], kink and soliton formation in lattices of coupled oscillators [11], and resonances in periodically forced oscillatory systems [12]. Particularly interesting contributions in this last category have been a number of recent experimental studies in periodically

forced chemical reaction-diffusion systems [13,14]. Perhaps the most challenging manifestation of pattern formation due to global modulation has occurred in granular materials, where vertically vibrated granular layers exhibit spatial and temporal patterning [8,15]. Our system differs from these others in one crucial respect, namely, that by itself each dynamic exhibits no interesting behavior and, in particular, no order, pattern formation, oscillatory behavior or instability of any kind. It is the alternation between uninteresting dynamics (generalizable to any periodic modulation) that is entirely responsible for the appearance of patterns in our model.

Our earlier work, based on a class of models associated with the Swift-Hohenberg equation [16,17], was mainly numerical. Herein we develop an analytic theory that captures, often quantitatively but in any case qualitatively, all the features of the pattern formation mechanism in all parameter regimes tested. The theory is based on a mode analysis of the nonlinear problem and the retention of only a few modes whose evolution reproduces the principal behavior of the system. Our detailed analysis is for a one-dimensional version of the model, for which we also present simulation results for comparison. These simulations complement our earlier two-dimensional simulations. We also outline the straightforward extension of our theory to two dimensions.

In Sec. II the general formalism, model system, and the important parameters of the problem are laid out. Section III presents the numerical simulation results for the one-dimensional version of the model. The analytic theory and its predictions are presented in Sec. IV, where comparisons with the numerical results are also detailed. We conclude with a short summary and discussion in Sec. V.

II. GENERAL FORMALISM

To illustrate the proposed mechanism, we consider a simple family of models that exhibit patterns. The overdamped Langevin dynamics for a scalar field $\varphi(\mathbf{r}, t)$ that depends on both space \mathbf{r} and time t reads in general

$$\dot{\varphi}(\mathbf{r},t) = -V'(\varphi(\mathbf{r},t)) + \mathcal{L}\varphi(\mathbf{r},t) + \xi(\mathbf{r},t). \quad (1)$$

The field could, for instance, represent the concentration of a chemical species at a given spatial position and time, or a scalar function of the velocity in a fluid. The temporal evolution of the field is driven by a local force that can be derived from a local potential $V(\varphi)$ by its coupling with other locations, indicated by the operator \mathcal{L} , and by fluctuations (for example, thermal fluctuations) modeled by the random term $\xi(\mathbf{r},t)$. We assume that $\xi(\mathbf{r},t)$ is Gaussian distributed, has zero mean value, and has a correlation function given by

$$\langle \xi(\mathbf{r},t)\xi(\mathbf{r}',t') \rangle = \sigma^2 \delta(\mathbf{r}-\mathbf{r}') \delta(t-t'). \quad (2)$$

A system such as (1) must satisfy two requirements for pattern formation: it must exhibit local multistability, that is, the local potential must have at least two stable equilibrium points, and it must have a morphological instability [16], i.e., $|\mathbf{k}|=0$ cannot be the most unstable Fourier mode. A paradigmatic example is a phenomenological model for the Rayleigh-Benard system near the convection threshold: the Swift-Hohenberg (SH) model [17]. A brief review of this model should be useful to clarify the features of the mechanism we are about to present.

For the SH model the local potential and the coupling term read, respectively,

$$V_{\text{SH}}(\varphi) = \frac{1}{4}\varphi^4 - \frac{a}{3}\varphi^3 - \frac{b}{2}\varphi^2, \quad (3)$$

$$\mathcal{L}_{\text{SH}} \equiv -(1 + \nabla^2)^2.$$

Note that the coupling operator determines an I_s morphological instability according to the classification criteria of Cross and Hohenberg [16], with $|\mathbf{k}^*|=1$ as the most unstable Fourier mode. Throughout this paper we will consider the coupling \mathcal{L}_{SH} . As for the local potential, we can distinguish different cases according to the value of the parameters a and b . If $a=0$ and $b \leq 0$, or if $a \neq 0$ and $b=0$, $V_{\text{SH}}(\varphi)$ has a single stable equilibrium point, and the system therefore does not develop (heterogeneous) patterns. For all other cases a spatial structure develops; its shape depends on dimensionality and on the symmetries satisfied by Eq. (1). If $a=0$ and $b > 0$, the local potential has two stable equilibrium points and is symmetric with respect to the line $\varphi=0$. Equation (1) is then invariant under the transformation $\varphi \leftrightarrow -\varphi$, and in two dimensions the system shows the rolls that are characteristic of the stationary structures associated with convection. On the other hand, if a and b are different from zero, $V_{\text{SH}}(\varphi)$ still exhibits two stable equilibrium points but the inversion symmetry $\varphi \leftrightarrow -\varphi$ is no longer satisfied by the evolution equation. In this case a two-dimensional system shows localized stationary spots arranged in a hexagonal lattice pattern.

According to this discussion, if $V(\varphi)$ is monostable no patterns appear, and the steady state of the system is spatially homogeneous. The homogeneous state is determined by the equilibrium point $\tilde{\varphi}$ of the *effective* local potential

$$\tilde{V}(\varphi) = V(\varphi) + \frac{\varphi^2}{2}. \quad (4)$$

The term $\varphi^2/2$ comes from the “1” in the coupling term acting on the field [see Eq. (3)]. That is, $\tilde{\varphi}$ is the solution of

$$V'(\tilde{\varphi}) + \tilde{\varphi} = 0. \quad (5)$$

Note that although $V(\varphi)$ is monostable, $\tilde{V}(\varphi)$ may not be, and then one may wonder about the possibility of generating a pattern, despite the fact that the local potential has only one equilibrium point. However, this will not occur: by considering small fluctuations around the homogeneous state, $\varphi = \tilde{\varphi} + \delta$, and linearizing Eq. (1), the following evolution equation for the Fourier component (indicated by a hat) of the field for the most unstable modes \mathbf{k}^* is obtained:

$$\hat{\delta}(\mathbf{k}^*,t) = -V''(\tilde{\varphi})\hat{\delta}(\mathbf{k}^*,t), \quad (6)$$

which leads to unstable behavior only if $V''(\tilde{\varphi}) < 0$. Since $V(\varphi)$ has only one equilibrium point, it follows that $V''(\tilde{\varphi}) > 0$ and thus no pattern arises even if $\tilde{V}(\varphi)$ is not monostable. Moreover, it may happen that $V(\varphi)$ and $\tilde{V}(\varphi)$ are *not* monostable, yet no structure develops because $V''(\tilde{\varphi}) > 0$. Hence we arrive at the following conditions:

$$\text{if } V'(\tilde{\varphi}) + \tilde{\varphi} = 0, \text{ but}$$

$$V''(\tilde{\varphi}) > 0, \text{ then no pattern develops;} \quad (7a)$$

$$\text{if } V'(\tilde{\varphi}) + \tilde{\varphi} = 0 \text{ and}$$

$$V''(\tilde{\varphi}) < 0, \text{ then a pattern develops.} \quad (7b)$$

Consider now a *global* switching mechanism between two local potentials $V_1(\varphi)$ and $V_2(\varphi)$:

$$\dot{\varphi}(\mathbf{r},t) = -\Lambda(t)V_1'(\varphi(\mathbf{r},t)) - [1 - \Lambda(t)]V_2'(\varphi(\mathbf{r},t)) + \mathcal{L}\varphi(\mathbf{r},t) + \xi(\mathbf{r},t). \quad (8)$$

Here $\Lambda(t)$ is a dichotomous function of time that takes on the values 0 and 1. In this way either $V_1(\varphi)$ or $V_2(\varphi)$ acts on the system at *every* site at a given time. It is easy to check that Eq. (8) can be rewritten as

$$\dot{\varphi}(\mathbf{r},t) = -V_+'(\varphi(\mathbf{r},t)) - \mu(t)V_-'(\varphi(\mathbf{r},t)) + \mathcal{L}\varphi(\mathbf{r},t) + \xi(\mathbf{r},t), \quad (9)$$

where

$$V_{\pm}(\varphi) \equiv \frac{V_1(\varphi) \pm V_2(\varphi)}{2} \quad (10)$$

and $\mu(t) = 2\Lambda(t) - 1 = \pm 1$.

Let us assume that $V_{1,2}(\varphi)$ and $\tilde{V}_{1,2}(\varphi)$ are *monostable* potentials. It is then clear according to conditions (7) that neither of the two dynamics alone will lead to patterns. How-

ever, we will show that the nonequilibrium process of alternation in time, either periodically or randomly, of two nonlinear dynamics neither of which leads to patterns, may lead to different kinds of oscillatory and stationary patterns.

Let t_s denote the average time that the system spends in each dynamics. Then we expect that if $t_s \rightarrow \infty$, that is, if switching is slow, every site will reach the equilibrium point $\tilde{\varphi}_i$ appropriate to the potential $V_i(\varphi)$ that drives the system. Therefore the field will oscillate between homogeneous structures. However, if the switching process is sufficiently fast (later we will state the condition quantitatively), the fast variable $\mu(t)$ can be replaced by its average value, $\mu(t) \sim \langle \mu(t) \rangle = 0$. Therefore in that limit the system is *effectively* driven by the potential $V_+(\varphi)$. We stress that although $V_{1,2}(\varphi)$ are monostable and satisfy the condition (7) associated with *no* pattern formation, $V_+(\varphi)$ may in general satisfy either condition. In particular, if $V_{1,2}(\varphi)$ are such that

$$V'_i(\tilde{\varphi}_i) + \tilde{\varphi}_i = 0 \quad \text{and} \quad V''_i(\tilde{\varphi}_i) > 0, \quad (11)$$

$$V'_+(\tilde{\varphi}_+) + \tilde{\varphi}_+ = 0 \quad \text{and} \quad V''_+(\tilde{\varphi}_+) < 0, \quad (12)$$

pattern formation will occur due to the *global* temporal alternation of two dynamics, neither of which alone leads to patterns.

Next we show that nonlinearity is needed for such a pattern formation mechanism. Consider for a moment the quadratic local potentials, that is, *linear* local forces, $V'_i(\varphi) = C_i\varphi - D_i$, where C_i and D_i are constants. Since we want these local potentials to satisfy Eq. (11), we must have $C_i > 0$. Obviously $V''_+(\varphi) = (C_1 + C_2)/2 > 0$, which allows no pattern according to Eq. (12). We must thus conclude that pattern formation by the mechanism described herein is only possible with nonlinear forces.

Given any particular choice of $V_{1,2}(\varphi)$ satisfying Eqs. (11) and (12), the formation of spatial structures can be understood in terms of the ratio r of the two characteristic times of the system: the time that the system spends in each dynamics, t_s , and the relaxation time to equilibrium states, t_r ,

$$r = \frac{t_s}{t_r}. \quad (13)$$

The time t_r is the smaller of $t_{1 \rightarrow 2}$ and $t_{2 \rightarrow 1}$, where $t_{i \rightarrow j}$ is the relaxation time, *under the action of* V_j , of the homogeneous state associated with V_i . We can estimate $t_{i \rightarrow j}$ by focusing only on the $|\mathbf{k}| = 0$ mode and assuming that, when the potential switches from V_i to V_j , the mode amplitude behaves as a Brownian particle initially equilibrated in the effective local potential $\tilde{V}_i(\varphi)$. When the local potential is switched, this point, which up to that moment was stable, becomes unstable. The relaxation time to the new homogeneous state associated with V_j is the time taken by the Brownian particle to roll down the potential hill to the new equilibrium point [18]:

$$t_{i \rightarrow j} = \frac{2}{\sigma^2} \int_{\tilde{\varphi}_i}^{\tilde{\varphi}_j} dy \exp\left(\frac{2}{\sigma^2} \tilde{V}_j(y)\right) \int_{\tilde{\varphi}_i}^y dz \exp\left(-\frac{2}{\sigma^2} \tilde{V}_j(z)\right). \quad (14)$$

The fluctuations should not dominate the dynamics, i.e., they must be small enough not to swamp the potential barrier in V_+ . Indeed, we might be tempted to approximate Eq. (14) by the deterministic limit,

$$t_{i \rightarrow j} = - \int_{\tilde{\varphi}_i}^{\tilde{\varphi}_j} \frac{dy}{\tilde{V}'_j(y)} + \mathcal{O}(\sigma^2). \quad (15)$$

Notice, however, that due to the absence of an inertial term in the model, Eq. (15) predicts the particle to be exponentially close to the equilibrium point $\tilde{\varphi}_j$ after a finite time but will only reach this point exactly in infinite time. For practical purposes, we can consider that the particle has “reached” the equilibrium point $\tilde{\varphi}_j$ when it is located at a distance of $\mathcal{O}(\sigma^2)$ from this point, so that the time $t_{i \rightarrow j}$ can, in fact, be estimated by Eq. (15) if the upper limit is replaced by $\tilde{\varphi} + \mathcal{O}(\sigma^2)$ [$\tilde{\varphi} - \mathcal{O}(\sigma^2)$] if the particle moves from right to left [left to right]. Moreover, if $\tilde{V}'_j(\varphi_i)$ varies little in the interval $(\tilde{\varphi}_i, \tilde{\varphi}_j)$ we arrive at the convenient estimate

$$t_{i \rightarrow j} \approx \frac{\tilde{\varphi}_i - \tilde{\varphi}_j}{V'_j(\tilde{\varphi}_i) + \tilde{\varphi}_i}. \quad (16)$$

Note that this last expression does not diverge as does Eq. (15) since $V'_j(\tilde{\varphi}_i) + \tilde{\varphi}_i \neq 0$.

On the other hand, the time that the system spends in one of the two dynamics, t_s , reads as follows. If the dichotomous switching is periodic, t_s is clearly the semiperiod of the signal, $t_s = T/2$. If the switching is random, we take $\Lambda(t)$ to be a dichotomous exponentially correlated random variable with correlation time τ . The correlation function of the associated random dichotomous variable $\mu(t)$ then is

$$\langle \mu(t) \mu(t') \rangle = e^{-|t-t'|/\tau}. \quad (17)$$

The time that the system spends in each dynamics on average is then $t_s = 2\tau$.

As commented above, if $r \gg 1$, the system will alternate between homogeneous states, and if $r \ll 1$, a stationary pattern will be obtained. The case $r \sim 1$ is the most striking; when the switching is periodic, a resonance phenomenon between the two characteristic times of the system may produce oscillatory patterns. These patterns only occur under periodic switching, that is, random switching even with a ratio $r \sim 1$ does not produce *sustained* oscillatory patterns. Although when $r \approx 1$ a collective oscillatorylike pattern may be found during a certain temporal window in the randomly switched system, the probability that $\mu(t)$ retains a given value for a time t longer than t_r is appreciable [$\mathcal{O}(e^{-t/t_r})$]. During such an event the whole system can relax to a homogeneous state. Once a homogeneous state is reached (and it

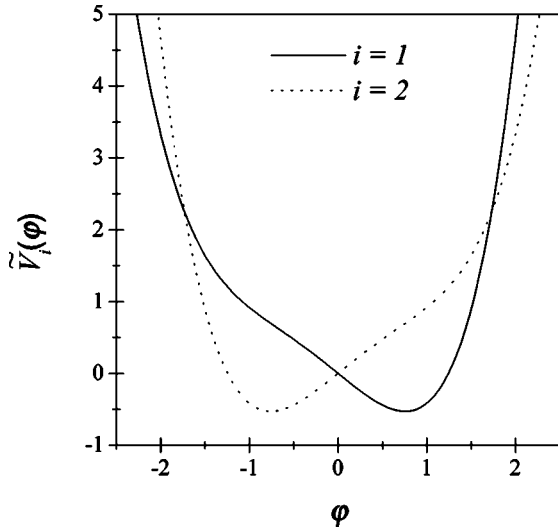


FIG. 1. Effective local potentials $\tilde{V}_1(\varphi)$ (solid curve) and $\tilde{V}_2(\varphi)$ (dotted curve) with $A_1=A_2=1$. The mirror symmetry is broken if $A_1 \neq A_2$.

will, sooner or later), it is very difficult for the system to recreate an oscillatory pattern. Periodic switching clearly bypasses this difficulty.

III. A PARTICULAR CASE: NUMERICAL SIMULATIONS

Let us now focus on the following particular family of local potentials that satisfy the conditions (11) and (12):

$$V_{1,2}(\varphi) = A_{1,2} \left(\frac{\varphi^4}{4} \pm \frac{\varphi^3}{3} - \frac{\varphi^2}{2} \mp \varphi \right), \quad (18)$$

where $A_{1,2}$ are positive constants. Then the potentials $V_{\pm}(\varphi)$ are

$$V_{\pm}(\varphi) = a_{\pm} \frac{\varphi^4}{4} + a_{\mp} \frac{\varphi^3}{3} - a_{\pm} \frac{\varphi^2}{2} - a_{\mp} \varphi, \quad (19)$$

where

$$a_{\pm} = \frac{A_1 \pm A_2}{2}. \quad (20)$$

There are two different cases according to the values of $A_{1,2}$. One is the symmetric case, $A_1=A_2$, for which $V_1(\varphi) = V_2(-\varphi)$. Since it then follows that $V_+(\varphi)$ is an even function of φ , the inversion symmetry $\varphi \leftrightarrow -\varphi$ is satisfied by Eq. (9) in the limit $r \rightarrow 0$. Away from this limit, the equation is invariant under the transformation combination $\{\varphi \leftrightarrow -\varphi, \mu \leftrightarrow -\mu\}$. The other is the asymmetric case, $A_1 \neq A_2$, for which the inversion symmetry is never satisfied. We restrict our simulations to the representative cases $A_1 = A_2 = 1$ and $A_1 = 1, A_2 = 2$ (see Fig. 1).

We first compute the relaxation time t_r . Using Eq. (14) with $\sigma^2 = 10^{-2}$, we obtain

$$t_r \approx 2.2 \quad \text{when } A_1 = A_2 = 1,$$

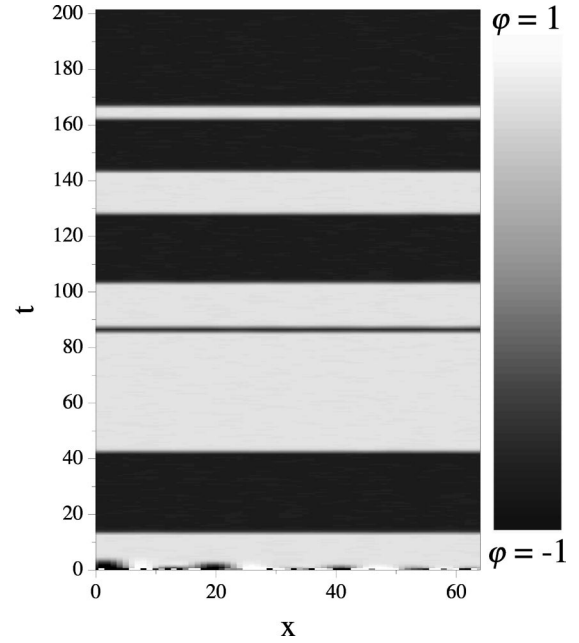


FIG. 2. Spatiotemporal density plot of the field for the 1D symmetric case $A_1=A_2=1$ with slow random switching ($r=4.5$). A clear alternation of homogeneous states is observed.

$$t_r \approx 1.3 \quad \text{when } A_1 = 1, \quad A_2 = 2. \quad (21)$$

These values are in agreement with those found in numerical experiments: $t_r = 2.49 \pm 10^{-2}$ and $t_r = 1.386 \pm 10^{-3}$, respectively. The approximate expression (16) yields $t_r \approx 1.8$ and $t_r \approx 1.7$, respectively.

In earlier work [6,7] we performed two-dimensional (2D) numerical simulations of Eq. (8) on 128×128 lattices with the local potentials (18). There we showed that stationary patterns of appropriate symmetries are indeed observed for $r \ll 1$ and oscillatory patterns are seen when $r \approx 1$. Here we perform complementary one-dimensional (1D) simulations. The values of the relevant parameters are $\Delta t = 10^{-3}$, $\Delta x = 0.5$, $L_x = 64$, and $\sigma = 10^{-2}$. In order to avoid possible instabilities arising from boundary effects we implement periodic boundary conditions. As in the 2D case, we expect the typical wavelength of the pattern to be $\lambda = 2\pi/|\mathbf{k}^*| \approx 2\pi$ and the aspect ratio to be $L/\lambda \sim 10$; that is, if a pattern develops, we expect to find ten wavelengths inside the lattice. These simulation results are compared to detailed theoretical results in the following section.

The initial condition is taken to be random according to a Gaussian distribution. As for the effect of the additive fluctuations in the dynamics, only if the initial condition were chosen to be uniform [$\varphi(\mathbf{r}, 0) = \text{const}$ for all \mathbf{r}] would they be relevant, since in all other cases small fluctuations do not play a significant dynamical role. Clearly, a uniform initial condition does not produce patterns in the deterministic problem regardless of the value of the control parameter r .

In Figs. 2 and 3 we show the results of typical simulations for the symmetric 1D case with random switching. We present a density plot of the field as a function of space and

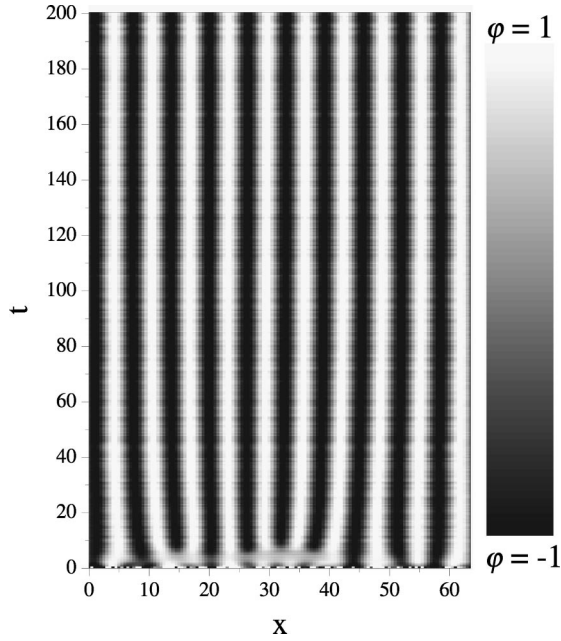


FIG. 3. Spatiotemporal density plot of the field for the 1D symmetric case $A_1=A_2=1$ with fast random switching ($r=0.045$). The system is essentially driven by the potential V_+ , and a stationary pattern develops.

time for $r=4.5$ (Fig. 2, slow switching) and $r=0.045$ (Fig. 3, fast switching). In the first case, a clear alternation between homogeneous states is obtained, and in the second we see the formation of a stationary pattern.

Deterministic periodic switching leads to results similar to those of random switching when $r \gg 1$ (alternation of homogeneous states) and $r \ll 1$ (stationary patterns). However, when $r \approx 1$ an oscillatory pattern develops. Figure 4 shows, again by means of a density plot of the field as a function of space and time, the oscillatory structure that arises when $r=1.15$. Below we will explain in detail the spatiotemporal structure of this oscillatory pattern.

The 1D asymmetric cases ($A_1 \neq A_2$), periodically or randomly switched, differ only in minor details from the symmetric cases.

We recall [6] that for the 2D system, different symmetries determine the spatial arrangements and shapes of patterns. For the symmetric case, $V_+(\varphi)$ is exactly the SH potential mentioned earlier, Eq. (3), with $a=0$ and $b>0$. Therefore, drawing parallels with that model, one expects and indeed observes stationary roll-shaped patterns in the limit $r \rightarrow 0$, since Eq. (9) satisfies the inversion symmetry (whether the alternation between dynamics is random or periodic). On the other hand, if $r \rightarrow \infty$, alternation between homogeneous states ensues, just as in the one-dimensional case. When the switching is deterministic, the main difference is the existence of sustained oscillatory patterns when $r \approx 1$. Since in that case the contribution of $V_-(\varphi)$ can no longer be neglected, the inversion symmetry is not satisfied by Eq. (9), whether $\mu=1$ or $\mu=-1$. Therefore, as in the SH model, a spotlike pattern emerges. However, Eq. (9) is invariant under the combined transformation $\{\varphi \leftrightarrow -\varphi, \mu \leftrightarrow -\mu\}$. This leads to a square arrangement of the oscillatory pattern, that

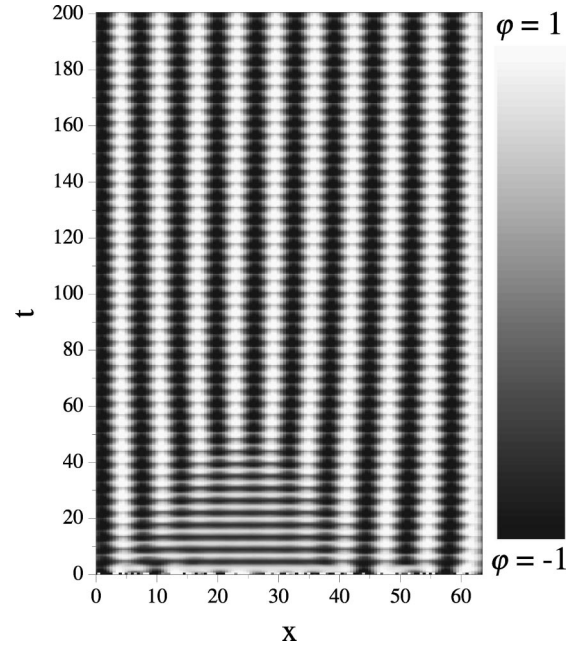


FIG. 4. Simulation results showing the 1D oscillatory patterns in the spatiotemporal evolution of the field for the symmetric case $A_1=A_2=1$. Switching is periodic with $r=1.15$. Figure 9 shows a single spatial and temporal period of such a pattern.

is, the spotlike structure presents a $\pi/2$ rotational symmetry and oscillates between the two possible square-glide-transformed lattices.

For the asymmetric case, again no spatial structure develops when $r \gg 1$, and one obtains a simple alternation in time of homogeneous states. The case $r \ll 1$ leads to a hexagonal stationary pattern, whether the switching is random or periodic. This is also the pattern that emerges in the 2D SH model in the absence of $\varphi \leftrightarrow -\varphi$ symmetry. When alternation is periodic, the case $r \approx 1$ leads to a hexagonal oscillatory pattern. Here there are no symmetry requirements to force alternation between glide-transformed lattices. Instead, we obtain truly localized excitations that resemble the oscillons found in *shaken* granular materials and clay. Figure 5 shows several snapshots over one period for $A_1=1$, $A_2=2$, and $r=0.95$. The hexagonal oscillatory pattern is clearly seen.

IV. MODE AMPLITUDE EQUATIONS

We now present a theoretical approach to the problem in terms of mode amplitude equations. For simplicity, and because the most interesting features of the problem occur even there, we restrict most of our calculations to the one-dimensional case. Moreover, since the periodic switching case captures the whole phenomenology of the pattern formation mechanism, we limit the calculations to that case.

Let us consider the following variant of our particular choice of local potentials (18):

$$V_{1,2}(\varphi) = A_{1,2} \left(\varepsilon \frac{\varphi^4}{4} \pm \gamma \frac{\varphi^3}{3} - \alpha \frac{\varphi^2}{2} \mp \varphi \right), \quad (22)$$

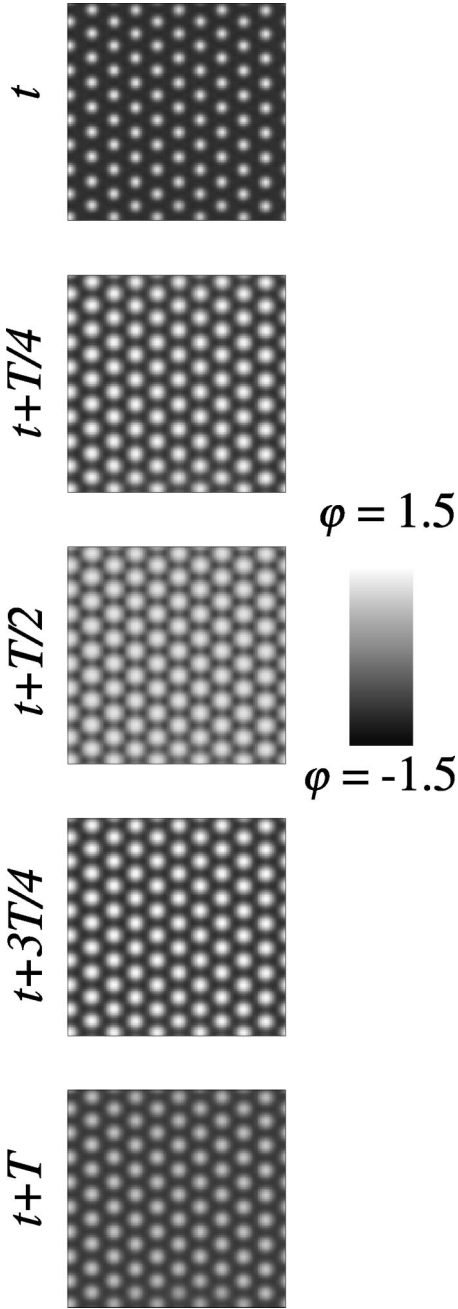


FIG. 5. Snapshots of the 2D field for the asymmetric case with $A_1=1$, $A_2=2$, and $r=0.94$ through a full period of the forcing function. The localized excitations are arranged in a hexagonal pattern.

where we have introduced the parameters α , ε , and γ in the nonlinear terms of the potential. For the moment, we will consider these parameters to be small [$\mathcal{O}(\alpha)=\mathcal{O}(\varepsilon)=\mathcal{O}(\gamma)$], and such that $V_i(\varphi)$ and $V_+(\varphi)$ satisfy the required stability conditions (11) and (12) for pattern formation under alternation of dynamics. Since the limits $r \gg 1$ and $r \ll 1$ will, respectively, produce alternation between homogeneous states and stationary patterns with typical wavelength $\lambda = 2\pi/k^* = 2\pi$, the most unstable modes will be $k=0$ and $k=k^*=1$ as we move from one limit to the other, that is, we expect solutions dominantly of the form

$$\varphi(x,t)|_{r \gg 1} = A_0(t),$$

$$\varphi(x,t)|_{r \ll 1} = A_1(t)e^{ix} + A_1^*(t)e^{-ix}. \quad (23)$$

However, the phenomenology observed in the oscillatory patterns is not well described by considering only these two modes or a linear combination of them. In order to reproduce these structures it is necessary to include the first Fourier spatial harmonic of k^* , i.e., $k=2k^*$, which arises from non-linear interactions. Hence we introduce the following ansatz for the field:

$$\varphi(x,t) = A_0(t) + \sum_{n=1}^2 [A_n(t)e^{inx} + A_n^*(t)e^{-inx}]. \quad (24)$$

Substituting Eq. (24) into Eq. (9) and neglecting all terms of order e^{inx} with $|n| \geq 3$, we obtain the following evolution equations for the mode amplitudes $A_0(t)$, $A_1(t)$, and $A_2(t)$ [\pm corresponds to the dichotomous variable taking on the value $\mu(t) = \pm 1$]:

$$\begin{aligned} \dot{A}_0 = & [\alpha(a_+ \pm a_-) - 1]A_0 + (a_- \pm a_+) - \varepsilon(a_+ \pm a_-) \\ & \times (6|A_1|^2 A_0 + 6|A_2|^2 A_0 + 3A_1^2 A_2^* + 3A_1^{*2} A_2 + A_0^3) \\ & - \gamma(a_- \pm a_+)(A_0^2 + 2|A_1|^2 + 2|A_2|^2), \end{aligned} \quad (25)$$

$$\begin{aligned} \dot{A}_1 = & \alpha(a_+ \pm a_-)A_1 - 3\varepsilon(a_+ \pm a_-)(|A_1|^2 A_1 \\ & + A_0^2 A_1 + 2|A_2|^2 A_1 + 2A_0 A_1^* A_2) \\ & - 2\gamma(a_- \pm a_+)(A_0 A_1 + A_1^* A_2), \end{aligned} \quad (26)$$

$$\begin{aligned} \dot{A}_2 = & [\alpha(a_+ \pm a_-) - 9]A_2 - 3\varepsilon(a_+ \pm a_-)(2|A_1|^2 A_2 \\ & + A_0^2 A_2 + |A_2|^2 A_2 + A_0 A_1^2) \\ & - \gamma(a_- \pm a_+)(A_1^2 + 2A_0 A_2). \end{aligned} \quad (27)$$

We assume that the A_j can be expanded in the parameters α , ε , and γ ,

$$A_j = A_j^{(0)} + \kappa A_j^{(1)} + \mathcal{O}(\alpha^2, \varepsilon^2, \gamma^2), \quad (28)$$

where $\kappa = \mathcal{O}(\alpha, \varepsilon, \gamma)$. The leading order for the A_j then yields the equations:

$$\dot{A}_0^{(0)} = -A_0^{(0)} + (a_- \pm a_+). \quad (29)$$

$$\dot{A}_1^{(0)} = 0. \quad (30)$$

$$\dot{A}_2^{(0)} = -9A_2^{(0)}. \quad (31)$$

Equation (29) can be solved completely by requiring that A_0 should be a continuous T -periodic function. The result is

$$A_0^{(0)}(t) = \begin{cases} a_- + a_+ \{1 - e^{-t} [1 - \tanh(T/4)]\} & \text{if } t \in [0, T/2] \\ a_- - a_+ \{1 + e^{-t} [1 - \tanh(T/4) - 2e^{T/2}]\} & \text{if } t \in [T/2, T]. \end{cases} \quad (32)$$

The term $A_2^{(0)}$ relaxes to zero rapidly in the long-term temporal evolution, and hence we can neglect it. Under this assumption, the next order for A_2 reads

$$\dot{A}_2^{(1)} = -9A_2^{(1)} - (A_1^{(0)})^2 \left(\frac{3\varepsilon(a_+ \pm a_-)}{\kappa} A_0^{(0)} + \frac{\gamma(a_- \pm a_+)}{\kappa} \right). \quad (33)$$

As for A_1 , Eq. (30) indicates that we must consider its next order,

$$\begin{aligned} \dot{A}_1^{(1)} = & \frac{A_1^{(0)}}{\kappa} \{ \alpha(a_+ \pm a_-) - 3\varepsilon(a_+ \pm a_-)(|A_1^{(0)}|^2 + (A_0^{(0)})^2) \\ & - 2\gamma(a_- \pm a_+)A_0^{(0)} \}. \end{aligned} \quad (34)$$

At the same time, Eq. (30) suggests that a reasonable simplification is to neglect the temporal dependence of $A_1^{(1)}$ by substituting $\langle (A_0^{(0)})^2 \rangle$ for $(A_0^{(0)})^2$ and $\langle A_0^{(0)} \rangle$ for $A_0^{(0)}$:

$$\begin{aligned} \langle A_0^{(0)} \rangle &= \frac{1}{T} \int_0^T A_0^{(0)}(t) dt = a_-, \\ \langle (A_0^{(0)})^2 \rangle &= \frac{1}{T} \int_0^T (A_0^{(0)}(t))^2 dt \\ &= (a_-)^2 + (a_+)^2 \left(1 - \frac{4 \tanh(T/4)}{T} \right). \end{aligned} \quad (35)$$

Equations (33) and (34) can be solved completely by using the result (32) and requiring that A_2 should be a continuous T -periodic function. The resulting expression for $A_1(t)$ is

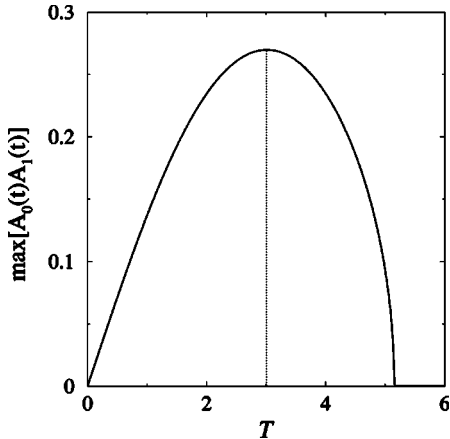


FIG. 6. The maximum in the resonance parameter A_0A_1 as a function of the period T gives the alternation period most likely to produce oscillatory patterns.

$$A_1(t) = \pm \text{Re} \left\{ \left[\frac{\alpha - 2\gamma|a_-|}{3\varepsilon} - (a_-)^2 + (a_+)^2 \left(\frac{4 \tanh(T/4)}{T} - 1 \right) \right]^{1/2} \right\} \quad \forall t. \quad (36)$$

We do not include the analytic expression for $A_2(t)$ because it is complex and not particularly illuminating. We do note that it can be written in the form

$$A_2(t) = A_1^2(t)F(t), \quad (37)$$

where $F(t)$ is a continuous T -periodic function. Therefore, if $A_1(t) \rightarrow 0$, then also $A_2(t) \rightarrow 0$.

Despite the fact that the theory is perturbative in the parameters α , ε , and γ , and so are the expressions (32), (36), and (37), we argue that the results can be applied at least qualitatively even when $\alpha = \varepsilon = \gamma = 1$, that is, to the local potentials used in the numerical simulations. We again begin by first discussing the symmetric case, $A_1 = A_2 = 1$, i.e., $a_+ = 1$, $a_- = 0$. In the limit $r \ll 1$ we expect a stationary pattern, such as $\varphi(x, t) = A_1 \cos x$; hence the mode amplitudes $A_0(t)$ and $A_2(t)$ must go to zero, as actually occurs in the theory. Moreover, in that limit Eq. (26) reduces to the Stuart-Watson equation [19], and the steady state of $A_1(t)$ can be *exactly* computed:

$$A_1 = 1/\sqrt{3}, \quad (38)$$

which is exactly the value found using the approximate equation (36). At the other extreme, in the limit $r \gg 1$ we expect $A_1(t)$ and $A_2(t)$ to go to zero since the system alternates between homogeneous states. That is the case for Eqs. (36) and (37). Also note that Eq. (32) indicates that $\varphi(x, t)$ indeed switches between $-a^{(+)} = -1$ and $a^{(+)} = 1$ for all x .

Oscillonlike patterns are expected in the intermediate regime, where both alternation and spatial structure are relevant. Therefore the quantity

$$\max[A_1(t)A_0(t)] \quad \text{for } t \in (0, T) \quad (39)$$

as a function of T estimates the regime where oscillatory patterns are most likely to appear. We represent Eq. (39) in Fig. 6. The maximum of the function is around $T \sim 3$. We take this value of the period to be the resonance value of the two characteristic times involved in the system, i.e., $r \approx 1$, so that $t_r \sim 1.5$. This value is in agreement with the one already found in numerical simulations and also in theoretical calculations.

We now compare the results found in the 1D numerical simulations with the theoretical predictions. The three panels in Fig. 7 depict the theoretical and numerical values obtained for $A_0(t)$, $A_1(t)$, and $A_2(t)$ for the cases $r \gg 1$, $r \approx 1$, and $r \ll 1$, respectively. In both theory and simulations, $A_0(t)$ os-

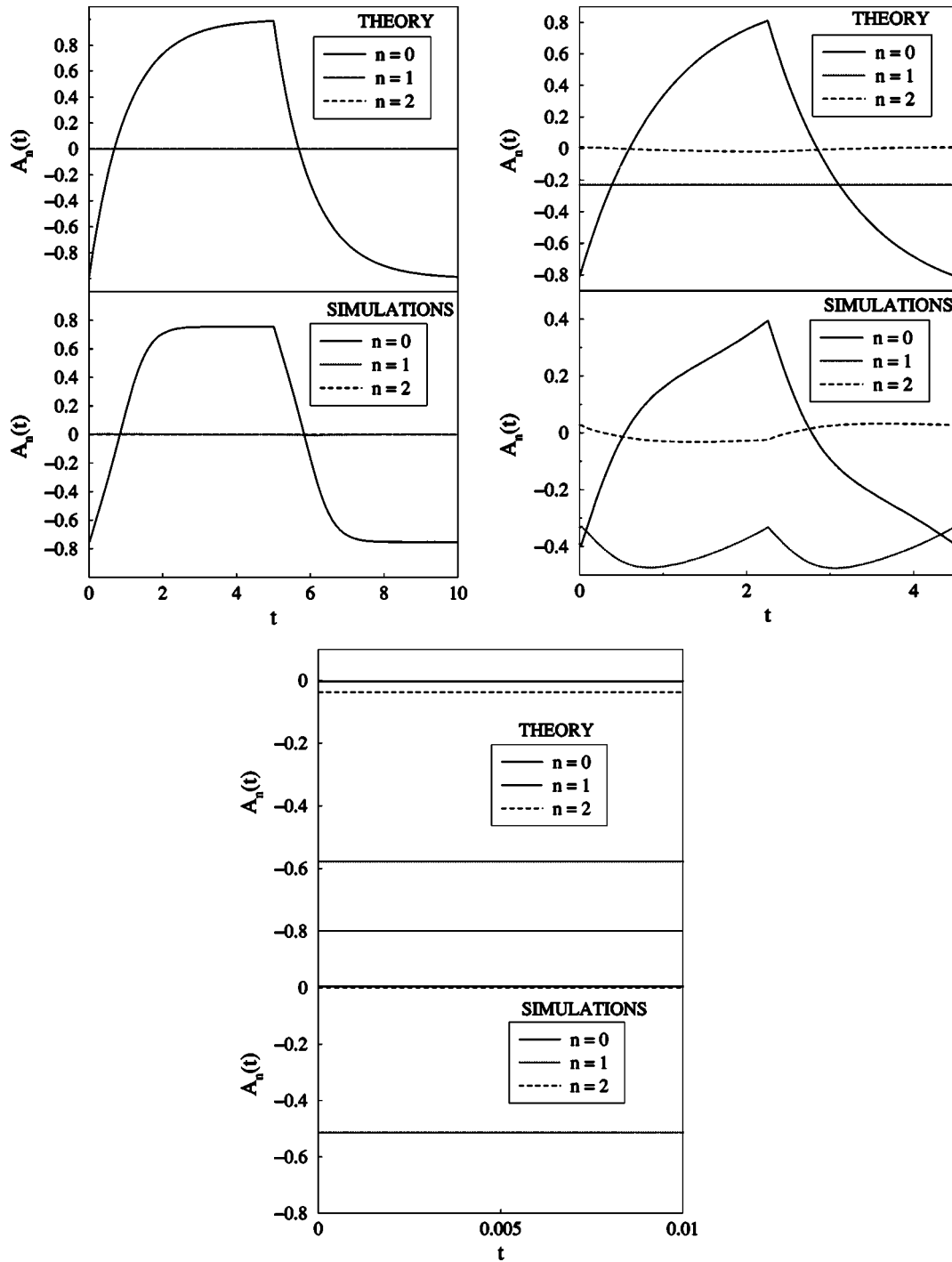


FIG. 7. Theoretical (upper portion of each panel) and numerical (lower portion) values of the coefficients of the three modes retained in the expansion, Eq. (24), for the cases $r \gg 1$ ($T=10$, first panel), $r \approx 1$ ($T=4.45$, second panel), and $r \ll 1$ ($T=10^{-2}$, third panel). In the first panel the only contribution to the dynamics comes from the $k=0$ mode, that is, homogeneous states alternating in time. In the third panel only the constant contribution of the $k=1$ mode becomes relevant, leading to a stationary pattern. The theoretical approach neglects the oscillations of the $A_1(t)$ mode, which are evident in the second panel.

cillates around zero with an amplitude that decreases and tends to zero as the period T decreases. The mode amplitude $A_2(t)$ fluctuates around zero in the regimes $r \ll 1$ and $r \gg 1$, and presents oscillations in the intermediate regime where oscillons are found. Finally, $A_1(t)$ shows a constant value if $r \ll 1$ or $r \gg 1$; however, in the intermediate oscillon regime,

$A_1(t)$ in the numerical simulations exhibits oscillations around a constant value. We have neglected these oscillations in our theoretical approach. They are not fundamental to the spatiotemporal behavior of $\varphi(x,t)$ as we will see below. We stress again that these comparisons between theory and simulations use perturbative theoretical expressions applied

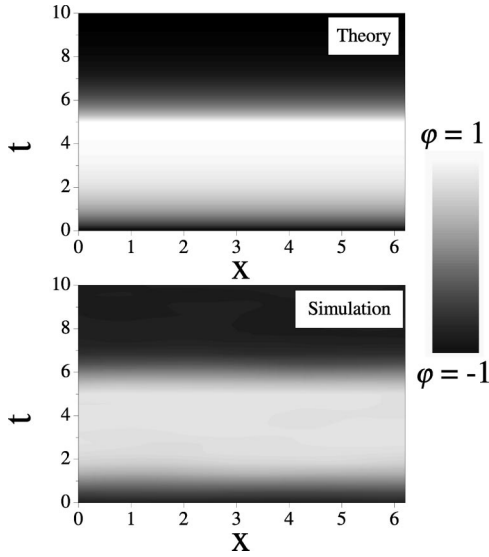


FIG. 8. Theoretical (upper panel) and numerical (lower panel) spatiotemporal density plot of $\varphi(x,t)$ for the symmetric case $A_1 = A_2 = 1$ with slow periodic switching ($T=10$, $r \gg 1$). The alternation of homogeneous states is captured quantitatively by the theory.

well beyond the perturbative regime. Nevertheless, the qualitative agreement is clear and becomes quantitative in the perturbative regime.

The qualitative agreement can be further ascertained by using Eq. (24) to reconstruct the field $\varphi(x,t)$. The results are shown in Figs. 8–10, where $\varphi(x,t)$ is depicted by means of density plots for the cases $r \gg 1$ (Fig. 8), $r \approx 1$ (Fig. 9), and $r \ll 1$ (Fig. 10). As said before, even when neglecting the oscillations of $A_1(t)$, the theory reproduces the behavior of the field as a function of the period. When $r \gg 1$ alternation between homogeneous states is obtained, and with $r \ll 1$ a

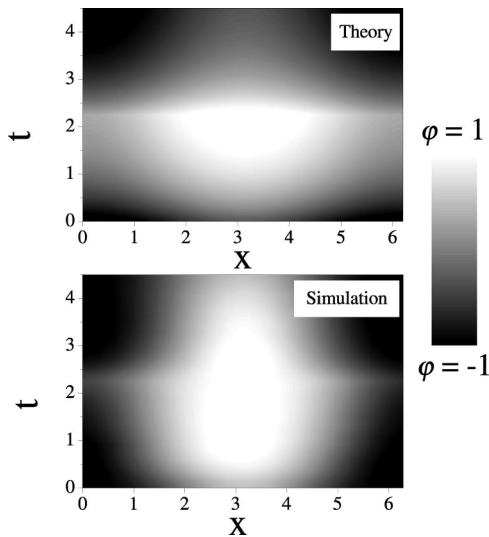


FIG. 9. Theoretical (upper panel) and numerical (lower panel) density plot of the field for the symmetric case with intermediate periodic switching ($T=4.5$, $r \approx 1$). The oscillatory pattern is captured qualitatively by the theory.

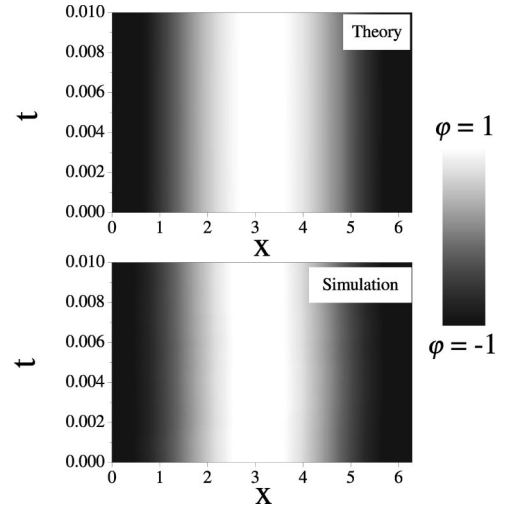


FIG. 10. Theoretical (upper panel) and numerical (lower panel) density plots of the field for the symmetric case with fast periodic switching ($T=10^{-2}$, $r \ll 1$). The stationary pattern is captured quantitatively by the theory.

stationary pattern appears. The agreement between theory and simulations is essentially quantitative. The intermediate regime $r \approx 1$ yields an oscillatory pattern in qualitative agreement with the pattern obtained from the simulations.

For the asymmetric case, $A_1 \neq A_2$, we briefly note that again theory and simulations agree qualitatively showing all the phenomenology as a function of the ratio r . The quantitative agreement, however, is not as good as in the symmetric case.

The spatial arrangement of the patterns obtained for the two-dimensional case can be inferred from our theory as follows. The structures arise from the nonlinear interactions between modes \mathbf{k}_j of magnitude $|\mathbf{k}_j| = k^* = 1$. Therefore, let us consider

$$\varphi(\mathbf{r}, t) = \sum_{|\mathbf{k}_j|=1} A_{1j} e^{i\mathbf{k}_j \cdot \mathbf{r}} + A_{1j}^* e^{-i\mathbf{k}_j \cdot \mathbf{r}}. \quad (40)$$

Substitution of Eq. (40) into Eq. (9) leads to the evolution equation for the modes A_{1j} [20]. We particularly highlight the following nonlinear mode interactions:

$$\text{Two modes: } (a_- \pm a_+) A_{1m} A_{1n}, \quad (41)$$

$$\text{Three modes: } (a_+ \pm a_-) A_{1j} A_{1j} A_{1j}^* \text{ modal self-interaction} \quad (42a)$$

$$\text{Three modes: } (a_+ \pm a_-) A_{1j} A_{1m} A_{1m}^* \text{ modal interaction.} \quad (42b)$$

The modes involved in the interactions (41) are those for which $\mathbf{k}_m + \mathbf{k}_n = \mathbf{k}_j$, that is, \mathbf{k}_m , \mathbf{k}_n , and \mathbf{k}_j lie apart by $\pi/3$. This favors a hexagonal pattern if the symmetries of the system support this pattern. The three-mode interactions, on the other hand, favor a square pattern or a roll pattern depending on the symmetries that must be fulfilled.

First consider the case $r \ll 1$ leading to stationary patterns. Since the adiabatic elimination of the fast variable, μ

$\rightarrow\langle\mu\rangle=0$, is equivalent to neglect of the \pm terms in Eqs. (41) and (42), it follows that the contribution of the two-mode interaction plays no role in the symmetric case since $a_- = 0$. The three-mode interactions must always be taken into account. In the symmetric case no particular regular arrangement arises from the three-mode interactions (42) because all the modes obey the inversion symmetry $\varphi \leftrightarrow -\varphi$. This then leads to a roll-shaped pattern. On the other hand, in the asymmetric case $a_- \neq 0$ and the inversion symmetry is no longer satisfied. The two-mode interaction (41) then becomes relevant. As a result, the pattern is hexagonal.

We now move to the case $r \approx 1$, i.e., oscillatory patterns. For the asymmetric case, the contribution of the two-mode interactions again leads to a hexagonal pattern, but now it oscillates in time. In the symmetric case, recall that the inversion symmetry, *together with* a time-translational symmetry, $t \rightarrow t + T/2$, is observed; that is, Eq. (9) remains invariant under the combined transformation $\{\varphi \leftrightarrow -\varphi, \mu \leftrightarrow -\mu\}$. Therefore the field oscillates between two glide-transformed structures. We note that if $\mu = 1$ or if $\mu = -1$ the system does not present inversion symmetry, so we expect a spotlike pattern for this oscillatory structure. However, the combined symmetry transformation forbids a hexagonal pattern. As a result, only the modal interactions wherein \mathbf{k}_m and \mathbf{k}_j are separated by $\pi/2$ are allowed, producing a square pattern that oscillates between the two possible glide-transformed structures.

V. DISCUSSION AND CONCLUSIONS

The global alternation of two dynamics, each of which leads to a homogeneous steady state, can produce stationary or oscillatory patterns upon alternation. The appearance of spatial or spatiotemporal patterns depends on the ratio r of the alternation time and the relaxation time of the system in the slower of the two dynamics. Random alternation leads to stationary spatial patterns, while periodic alternation may lead to stationary or oscillatory spatial patterns. The symmetry of the patterns depends on the symmetries of the potentials.

This mechanism for pattern formation was earlier illustrated through numerical simulations in a 2D system based on the Swift-Hohenberg equation [6,7]. Herein we have performed numerical simulations for the corresponding 1D system and have developed an analytic three-mode theory that

captures (in many cases even quantitatively) the behavior in all parameter regimes. The three modes that are included in this theory are the uniform mode ($k=0$), the most unstable mode ($k=k^*=1$), and the first Fourier spatial harmonic of this unstable mode ($k=2k^*$). The analytic results lead to periodic alternation of homogeneous states for large r , stationary patterns for small r , and in the case of periodic alternation to oscillatory patterns for intermediate r .

We have also outlined the way in which this theory can easily be extended to the 2D system, where more than three modes need to be considered. Here one has to include all modes with a wave vector of unit magnitude as well as a subset of two-mode and three-mode interactions that dominate the dynamics. The number of modes is still small and analytically tractable.

The alternation mechanism has thus been presented numerically and understood analytically for certain classes of models based on the Swift-Hohenberg equation. One can envision many other situations in which a global alternation between homogeneous or even chaotic dynamics may lead to spatiotemporal pattern formation. We stress again the most interesting aspect of this mechanism, namely, that the alternation is *global*. A parallel theory for an entirely different class of models of the reaction-diffusion type has been developed [21]. The minimal feature that is required for any alternation mechanism to lead to pattern formation is that the most unstable mode of the system corresponds to a nonzero eigenvector \mathbf{k} , whose magnitude determines the length scale of the pattern. In the Swift-Hohenberg-type model considered here this nonzero-wave-vector instability is due to the particular form of the coupling. In reaction-diffusion systems with ordinary diffusive coupling, one requires at least two coupled fields to obtain a nonzero-wave-vector instability [21].

ACKNOWLEDGMENTS

This work was partially supported by the National Science Foundation under Grant No. PHY-9970699, by a grant from the University of California, Institute for México and the United States (UC MEXUS), the Consejo Nacional de Ciencia y Tecnología de México (CONACYT), the *New Del Amo Program*, by MECD-Spain Grant No. EX2001-02880680, and by Grant No. BFM2001-0291.

-
- [1] P. Manneville, *Dissipative Structures and Weak Turbulence* (Academic, Boston, 1990); H. Mori and Y. Kuramoto, *Dissipative Structures and Chaos* (Springer, Berlin, 1998).
- [2] C. W. Meyer, D. S. Cannell, G. Ahlers, J. B. Swift, and P. C. Hohenberg, *Phys. Rev. Lett.* **61**, 947 (1988); D. Walgraef, *J. Stat. Phys.* **64**, 969 (1991).
- [3] C. Careta and F. Sagués, *J. Chem. Phys.* **92**, 1098 (1990); F. Drolet and J. Viñals, *Phys. Rev. E* **56**, 2649 (1997).
- [4] J. García-Ojalvo and J. M. Sancho, *Noise in Spatially Extended Systems* (Springer, New York, 1999); C. Van den Broeck, J. M. R. Parrondo, R. Toral, and R. Kawai, *Phys. Rev. E* **55**, 4084 (1997).
- [5] J. M. R. Parrondo, C. Van den Broeck, J. Buceta, and F. J. de la Rubia, *Physica A* **224**, 153 (1996).
- [6] J. Buceta, K. Lindenberg, and J. M. R. Parrondo, *Phys. Rev. Lett.* **88**, 024103 (2002).
- [7] J. Buceta, K. Lindenberg, and J. M. R. Parrondo *Fluct. Noise Lett.* **2**, L21 (2002).
- [8] P. B. Umbanhowar, F. Melo, and H. L. Swinney, *Nature (London)* **382**, 793 (1996).

- [9] J. Tan and G. Gabrielse, *Phys. Rev. Lett.* **67**, 3090 (1991).
- [10] N. Grønbech-Jensen, Y. S. Kivshar, and M. R. Samuelsen, *Phys. Rev. B* **47**, 5013 (1993); R. Grauer and Y. S. Kivshar, *Phys. Rev. E* **48**, 4791 (1993).
- [11] B. Denardo *et al.*, *Phys. Rev. Lett.* **68**, 1730 (1992); N. V. Alexeeva, I. V. Barashenkov, and G. P. Tsironis, *ibid.* **84**, 3053 (2000).
- [12] A. Chiffaudel and S. Fauve, *Phys. Rev. A* **35**, 4004 (1987); P. Coullet, J. Lega, B. Houchmanzadeh, and J. Lajzerowicz, *Phys. Rev. Lett.* **65**, 1352 (1990); C. Elphick, A. Hagberg, and E. Meron, *Phys. Rev. E* **59**, 5285 (1999).
- [13] V. Petrov, Q. Quyang, and H. L. Swinney, *Nature (London)* **388**, 655 (1997).
- [14] A. L. Lin, M. Bertram, K. Martinez, H. L. Swinney, A. Ardelea, and G. E. Carey, *Phys. Rev. Lett.* **84**, 4240 (2000); A. L. Lin, A. Hagberg, A. Ardelea, M. Bertram, H. L. Swinney, and E. Meron, *Phys. Rev. E* **62**, 3790 (2000).
- [15] S. C. Venkataramani and E. Ott, *Phys. Rev. E* **63**, 046202 (2001).
- [16] M. C. Cross and P. C. Hohenberg, *Rev. Mod. Phys.* **65**, 851 (1993).
- [17] J. Swift and P. C. Hohenberg, *Phys. Rev. A* **15**, 319 (1977).
- [18] C. W. Gardiner, *Handbook of Stochastic Methods*, 2nd ed. (Springer, Berlin, 1985); A. N. Malakhov, *Chaos* **7**, 488 (1997).
- [19] J. T. Stuart and R. DiPrima, *Proc. R. Soc. London, Ser. A* **362**, 27 (1978).
- [20] A. C. Newell, in *the Proceedings of the 1988 Complex Systems Summer School*, Lectures in the Sciences of Complexity Santa Fe, New Mexico, edited by D. L. Stein (Addison-Wesley, Reading, MA, 1989).
- [21] J. Buceta and K. Lindenberg, *Phys. Rev. E* (to be published).